

## Relative strength of the screened Coulomb interaction and phase-space filling on exciton bleaching in multiple quantum well structures

Moongoo Choi, Koo-Chul Je, Sang-Youp Yim, and Seung-Han Park\*

*National Research Laboratory of Nonlinear Optics, Yonsei University, Seoul 120-749, Korea*

(Received 5 April 2004; published 20 August 2004)

We investigate the effect of resonantly excited excitons on the bleaching of  $n=1$  and  $n=2$  heavy-hole (hh) exciton resonances in *GaAs* multiple-quantum-well structures by using a pump-probe spectroscopic technique at low temperature under quasi-stationary excitation conditions. In particular, we present direct observation of long-range Coulomb screening by two-dimensional exciton-exciton interactions along with the unambiguous discrimination of screened Coulomb interaction and phase-space filling on the  $n=1$  hh exciton bleaching. In addition, we find that the strength of long-range Coulomb screening on the  $n=1$  hh exciton bleaching is only two to three times weaker than that of the phase-space filling at 10 K.

DOI: 10.1103/PhysRevB.70.085309

PACS number(s): 78.67.De, 71.35.Cc

Quantum confinement effects in semiconductor multiple quantum wells (MQW's) enhance excitonic features, including strong and well-resolved excitonic peaks in linear absorption even at room temperature.<sup>1,2</sup> With increasing densities of photo-generated free electrons and holes, the excitonic absorption spectra are observed to be shifted, broadened, and saturated due to the Pauli exclusion principle, the screening of Coulomb interaction, band-gap renormalization, etc.<sup>3-5</sup> The exclusion principle, consisting of phase-space filling (PSF) and exchange effects, is very short ranged compared to the screened Coulomb interaction. Hereafter, we will denote the PSF and exchange effects as PSF.

During the past decades, relative contribution of Coulomb screening (CS) and PSF to the density-dependent exciton bleaching in bulk and MQW structures have been intensively investigated under various excitation conditions.<sup>6-13</sup> Fehrenbach *et al.*<sup>6</sup> observed that the screening of excitons by surrounding excitons is much weaker than that by free carriers in bulk *GaAs*. In *GaAs* MQW's, Knox *et al.*<sup>7</sup> found that resonantly generated excitons produce more absorption bleaching than free-carrier pairs of equal densities at room temperature. Recently, Becker *et al.*<sup>8</sup> showed that the bleaching effect of "cold" neutral excitons is stronger than that of the same density of "cool" uncorrelated charged electron-hole pairs in *CdZnTe/ZnTe* MQW's. However, to our knowledge, no experimental data on the long-range CS of excitons by excitons in quasi-two-dimensional (quasi-2D) MQW's have been available.

In this Letter, we report the first direct observation of long-range CS by two-dimensional exciton-exciton interactions as well as unambiguous discrimination of CS and PSF effects on the  $n=1$  heavy-hole (hh) exciton bleaching at low temperature ( $T=10$  K). In particular, we measured the changes of optical absorption for  $n=1$  hh and  $n=2$  hh exciton resonances simultaneously in a *GaAs/AlGaAs* MQW by using a pump-probe spectroscopic technique under quasi-stationary  $n=1$  hh excitation conditions with a narrow-band nano-second laser. We observed the absorption bleaching of  $n=1$  hh exciton resonance due to PSF and long-range CS, as expected. Surprisingly, however, we were also able to observe that neutral excitons generated at  $n=1$  hh induce the

bleaching of excitons at  $n=2$  hh, strongly indicating the presence of long-range CS in the quasi-two-dimensional system. We subtracted the variation of  $n=2$  hh from that of  $n=1$  hh in order to deduce the PSF effect on the  $n=1$  hh bleaching since the  $n=1$  hh absorption bleaching is caused by both PSF and long-range CS. From the data we find that the relative strength of the absorption bleaching effect by PSF is only two to three times stronger than that of long-range CS. It agrees well with estimates from our theoretical calculation based on the multi-band-semiconductor Bloch equations.<sup>5,14</sup>

Figure 1 shows the spectral shapes of the pump pulse, the broadband probe pulse, and the absorbance,  $\alpha L = -\ln(I_t/I_0)$ , of a *GaAs/AlGaAs* MQW at 10 K. Here,  $I_0$  and  $I_t$  are incident and transmitted intensities, respectively. The sample used in this study consists of 65 periods of 75 Å *GaAs* wells and 100 Å *Al<sub>0.34</sub>Ga<sub>0.66</sub>As* barriers grown by molecular beam epitaxy. The substrate was removed by selective etching over part of the sample in order to allow transmission measurements. The resulting sample had sufficiently good optical quality in the vicinity of the excitonic peaks. The well-defined  $n=1$  hh and  $n=2$  hh exciton peaks were observed at 1.5684 eV and 1.6994 eV with line widths of  $\sim 2.7$  meV and

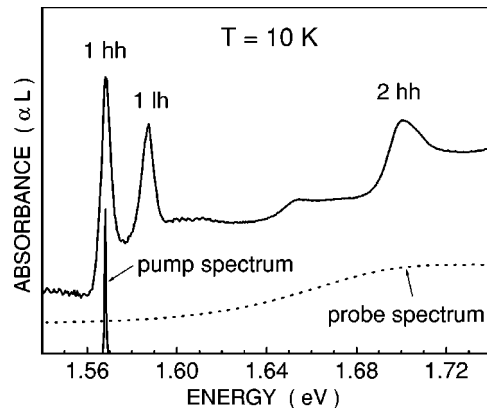


FIG. 1. Linear absorption spectrum of *GaAs/AlGaAs* MQW structure at 10 K, including the spectral shapes of the pump and probe pulses.

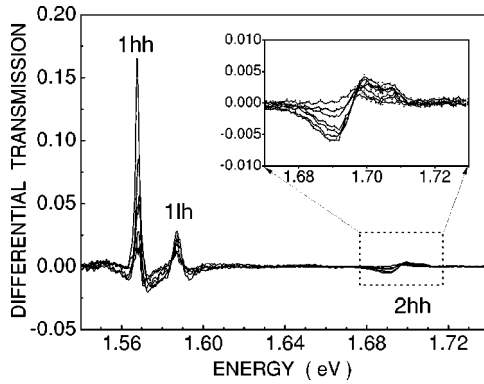


FIG. 2. Low temperature differential transmission spectra measured at both  $n=1$  hh and  $n=2$  hh excitons. The inset shows the enlarged view of differential transmission spectra near the  $n=2$  hh excitons.

$\sim 7.8$  meV, respectively. The peak around 1.587 eV corresponds to the  $n=1$  light-hole (lh) exciton.

The experiments were performed using a quasi-stationary pump and probe measurement technique. A Nd:YAG laser pumped dye-laser system operating at  $n=1$  hh exciton resonance with a repetition rate of 10 Hz was employed for the pump beam. The probe pulses with very low intensity spectrally cover both  $n=1$  hh and  $n=2$  hh exciton resonances, as shown in Fig. 1. The pump pulses were  $\sim 5$  ns in duration and the probe focus was kept much smaller than the size of the pump beam. A shutter synchronized with the laser pulse was used to get a high signal-to-noise ratio and remove the scattered laser beams. The transmission spectra with and without the pump beam were monitored using an optical multi-channel analyzer (OMA) with image sensing photodiode arrays.

Figure 2 shows the low temperature differential transmission spectra (DTS) which are taken near both  $n=1$  hh and  $n=2$  hh exciton resonances. The DTS is defined as  $DTS = (T - T_0)/T$ , where  $T$  is the probe transmission with the pump present and  $T_0$  is the probe transmission without the pump. The spectra show induced transmission variations, i.e., bleaching of various excitonic transitions. The peaks are caused by variations of oscillator strengths of the excitons, where the absolute value of the induced transmission becomes larger as the pump beam intensity increases. The DTS around the  $n=1$  hh excitonic resonance is positive, however, the high energy side of  $n=1$  hh is negative, which originates from spectral overlapping of  $n=1$  hh and  $n=11$  h resonances.

In addition, we also observe absorption bleaching near the  $n=2$  hh excitons, as is depicted in the inset of Fig. 2. It is worth noting that the wavelength of the pump beam is tuned at the  $n=1$  hh exciton resonance, the excited excitons are created by the pump pulse with  $\Delta E_{\text{Laser}} < 1.0$  meV (much smaller than the  $n=1$  hh exciton linewidth,  $\Delta E_{1\text{hh}} \sim 2.7$  meV) at 10 K, where the thermal-LO-phonon density is ignorable, and the decay time of excitons is the order of nanoseconds even at room temperature.<sup>15–17</sup> In order to minimize the effect of spectral hole burning due to the inhomogeneous broadening, in addition, the DTS were measured by

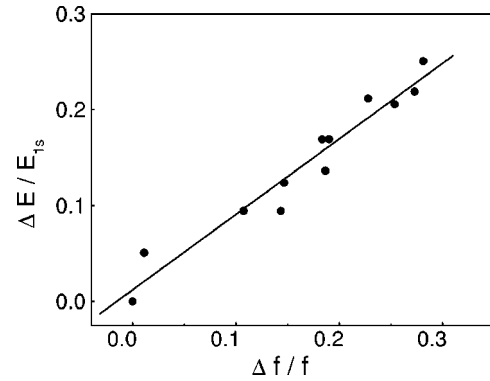


FIG. 3. The fractional change of exciton binding energy as a function of relative decrease of exciton oscillator strength.

controlling the intensity of the pump beam to create the carrier densities of up to  $1.4 \times 10^{11} \text{ cm}^{-2}$ . Since only the ground-state excitons in the first subband are generated, the  $n=2$  hh excitons in the second sub-band are affected solely by the long-range CS. In contrast to the  $n=1$  hh exciton, however, negative and positive DTS are obtained in the low and high energy sides of the  $n=2$  hh exciton, respectively. This means that the  $n=2$  hh excitonic absorption spectra are red-shifted for increased exciton density. Therefore, the experimental observation clearly indicates the existence of long-range CS effects in the quasi-2D systems.

There are mainly two many-body effects acting in opposite directions of the peak shifts; an attractive inter-particle interaction influenced by long-range CS and a repulsive interaction by PSF, which contribute to red and blue shifts, respectively.<sup>3,5,12</sup> As mentioned above, the  $n=2$  hh excitons are only affected by an attractive long range CS, exhibited by a red-shift of the  $n=2$  hh exciton resonance. On the contrary, the blue-shifted  $n=1$  hh exciton resonance is affected by both a repulsive PSF and an attractive long-range CS. These two opposite effects lead to the net change of the  $n=1$  hh exciton resonance. The observed blue shift of the  $n=1$  hh excitons indicates that PSF is stronger than long-range CS in a quasi-2D system. Note that both attractive and repulsive interactions also produce a reduction of excitonic oscillator strength. In summary, the long-range CS affects excitons of all sub-bands, whereas the PSF effects are restricted to the  $n=1$  hh excitons of the occupied sub-band.

Figure 3 displays the relation between the peak shift and bleaching of the  $n=1$  hh excitons due to PSF, which is given by  $(\Delta E/E_{1s}) = C(\Delta f_0/f_0)$ ,<sup>3,11,18</sup> where  $E_{1s}$  is a binding energy of bare  $n=1$  hh excitons and  $f_0$  is its oscillator strength. The magnitudes of  $\Delta f_0$  and  $\Delta E$  are determined by Gaussian fitting of nonlinear absorbance obtained by adding the DTS to the linear absorbance in Fig. 1. In particular, for an accurate comparison, we subtract the reduction ratio of oscillator strength in the  $n=2$  hh excitons due to long-range CS from that of the  $n=1$  hh excitons in order to eliminate the long range CS effect in the DTS. In addition, the net blue-shift of the  $n=1$  hh excitons due to only PSF is extracted by compensating the red-shift of the  $n=2$  hh excitons due to long-range CS with the observed blue-shift of the  $n=1$  hh excitons. As can be seen in Fig. 3, we find a good linear

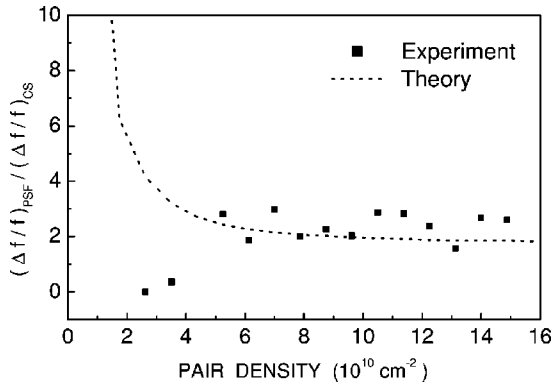


FIG. 4. Relative strength of PSF and CS on the  $n=1$  hh exciton bleaching for various excitation densities. The dashed line corresponds to the theoretical calculation.

correlation between the net fractional change of exciton binding energy and  $\Delta f_0/f_0$  for PSF. The coefficient  $C$  is obtained to be 0.8, which is 1.6 times larger than the predicted value. Nevertheless, it is comparable to previously reported experimental values of 0.3~1.0.<sup>11,18</sup> The coefficient  $C$  is known to be close to zero for 3D systems, while for 2D systems they have nonzero values dependent upon their well size.<sup>3,6,11,18</sup>

The experimental data points in Fig. 4 show the ratio of the contribution of PSF and CS on the  $n=1$  hh exciton bleaching for various excitation densities. It is found that the bleaching rate is almost constant between 2 and 3 with increasing carrier densities from  $3 \times 10^{10} \text{ cm}^{-2}$  to  $1.4 \times 10^{11} \text{ cm}^{-2}$ . In other words, bleaching due to PSF is nearly unvaried with values at around 2–3 times larger than that due to CS. In order to understand this behavior, we investigated the relative strength of bleaching effects due to CS and PSF theoretically by using the multi-band semiconductor Bloch equations onto the lowest  $1s$  exciton state. The nonlinear optical response of a semiconductor up to the third-order can be described by<sup>5</sup>

$$\left(-i\frac{\partial}{\partial t} - \Omega_0\right)P(t) = -\mu \cdot E(t) + b\mu \cdot E(t)|P(t)|^2 + vP(t)|P(t)|^2.$$

Here,  $\Omega_0$  is the frequency of the exciton resonance,  $\mu$  its transition dipole moment,  $E(t)$  the external laser field, and  $\mu P$  the interband polarization. Moreover,  $b=2\sum_{\vec{k}} \phi(\vec{k})^3$  represents a nonlinearity induced by Pauli blocking and  $v=2\sum_{\vec{k}} V_s(\vec{k}-\vec{k}')[\phi(\vec{k})^3\phi(\vec{k}') - \phi(\vec{k})^2\phi(\vec{k}')^2]$  is a nonlinearity

originating from the Coulomb interaction.  $\phi(\vec{k})$  is assumed to be a real wavefunction of the  $1s$  exciton and  $\vec{k}$  denotes the momentum associated with the relative motion of electrons and holes. The two terms, which determine  $v$ , are originated from the field renormalization and the band-gap renormalization in the full semiconductor Bloch equation. The screened two-dimensional Coulomb potential is assumed to be

$$V_s(\vec{k}-\vec{k}') = \frac{2\pi e^2}{\epsilon_0 L^2} \frac{1}{(\vec{k}-\vec{k}') + \kappa}, \quad (1)$$

treated statically using the plasmon-pole approximation.<sup>19,20</sup> The inverse of the screening length,  $\kappa$ , is calculated self-consistently according to  $\kappa^2 = (2\pi e^2/\epsilon_0 V)\sum_n [df_n(k)/d\epsilon]$ , where  $f_n(k)$  is the distribution function of the band index  $n$ , and  $\epsilon_0$  is the background dielectric constant. Within these approximations the explicit form of the third-order response is characterized by the ratio  $v/b$ , which determines the relative strength of the two sources of optical nonlinearity. We have ignored the light-hole states in our theoretical consideration. The calculated bleaching rate is shown in Fig. 4 as a dotted line. As can be seen in the figure, the bleaching due to PSF is estimated to be constant around 2 times larger than that due to CS within the carrier concentration  $2.0 \times 10^{11} \text{ cm}^{-2}$ .<sup>14</sup> We find that the theoretical calculations agree well with experimental results. However, the calculated bleaching rate shows a rapid increase for very low densities. This result is presumed to come from very small excitonic bleaching of the  $n=2$  hh peak due to CS in the very low densities, in which our calculations are limited.

In conclusion, we have found that the  $n=2$  hh exciton resonance is consistently red-shifted by two-dimensional exciton-exciton interactions in *GaAs/AlGaAs* MQW's under quasi-stationary  $n=1$  hh excitation conditions at low temperatures. This confirms that the effect of the excited excitons at  $n=1$  hh on excitons at  $n=2$  hh is primarily due to long-range CS, which is not negligible in the quasi-2D system. On the other hand, the  $n=1$  hh exciton resonance is blue-shifted by the competition of both repulsive PSF and attractive long-range CS, which should be compensated. After discriminating PSF and long-range CS effects in the  $n=1$  hh exciton bleaching, we find that the relative strength of absorption bleaching due to long-range CS is only 2 to 3 times weaker than that of PSF. The theoretically calculated value based on the multi-band semiconductor Bloch equations is in good agreement with our experimental results.

This research was supported by the Ministry of Science and Technology of Korea through the National Research Laboratory Program (Contract No. M1-0203-00-0082).

\*Electronic address: shpark@phya.yonsei.ac.kr

<sup>1</sup>D. S. Chemla, D. A. B. Miller, P. W. Smith, A. C. Gossard, and W. Wiegmann, *IEEE J. Quantum Electron.* **20**, 265 (1984).

<sup>2</sup>C. Weisbuch and B. Vinter, *Quantum Semiconductor Structures* (Academic, San Diego, 1991).

<sup>3</sup>S. Schmitt-Rink, D. S. Chemla, and D. A. B. Miller, *Phys. Rev. B* **32**, 6601 (1985).

<sup>4</sup>H. Haug and S. Schmitt-Rink, *J. Opt. Soc. Am. B* **2**, 1135 (1985).

<sup>5</sup>H. Haug and S. W. Koch, *Quantum Theory of the Optical and Electronic Properties of Semiconductors* (World Scientific, Sin-

- gapore, 1994).
- <sup>6</sup>G. W. Fehrenbach, W. Schafer, J. Treusch, and R. G. Ulbrich, *Phys. Rev. Lett.* **49**, 1281 (1982).
- <sup>7</sup>W. H. Knox, R. L. Fork, M. C. Downer, D. A. B. Miller, D. S. Chemla, and C. V. Shank, A. C. Gossard, and W. Wiegmann, *Phys. Rev. Lett.* **54**, 1306 (1985).
- <sup>8</sup>P. C. Becker, D. Lee, A. M. Johnson, A. G. Prosser, R. D. Feldman, R. F. Austin, and R. E. Behringer, *Phys. Rev. Lett.* **68**, 1876 (1992).
- <sup>9</sup>D. R. Wake, H. W. Yoon, J. P. Wolfe, and H. Morkoc, *Phys. Rev. B* **46**, 13 452 (1992).
- <sup>10</sup>E. Lach, M. Walther, G. Traenkle, A. Forchel, and G. Weimann, *Phys. Status Solidi B* **150**, 679 (1988).
- <sup>11</sup>K.-H. Schlaad, Ch. Weber, J. Cunningham, C. V. Hoof, G. Borghs, G. Weimann, W. Schlapp, H. Nickel, and C. Klingshirn, *Phys. Rev. B* **43**, 4268 (1991).
- <sup>12</sup>S. Hunsche, K. Leo, H. Kurz, and K. Kohler, *Phys. Rev. B* **49**, 16 565 (1994).
- <sup>13</sup>W. H. Knox, C. Hirlimann, D. A. B. Miller, J. Shah, D. S. Chemla, and C. V. Shank, *Phys. Rev. Lett.* **56**, 1191 (1986).
- <sup>14</sup>K.-C. Je, M. Choi, S.-Y. Yim, J.-S. Ahn and S.-H. Park, *Phys. Rev. B* **66**, 155312 (2002).
- <sup>15</sup>M. Colocci, M. Gurioli, and A. Vinattieri, *J. Appl. Phys.* **68**, 2809 (1990).
- <sup>16</sup>J. E. Fouquet and A. E. Siegman, *Appl. Phys. Lett.* **46**, 280 (1985).
- <sup>17</sup>W. Pickin and J. P. R. David, *Appl. Phys. Lett.* **56**, 268 (1990).
- <sup>18</sup>D. Hulin, A. Mysyrowicz, A. Antonetti, A. Migus, W. T. Masselink, H. Morkoc, H. M. Gibbs, and N. Peyghambarian, *Phys. Rev. B* **33**, 4389 (1986).
- <sup>19</sup>H. Haug and C. Ell, *Phys. Rev. B* **46**, 2126 (1992).
- <sup>20</sup>K.-C. Je, K.-C. Seo and Y. Kim, *J. Appl. Phys.* **86**, 6196 (1999).